

# Learning to Optimize for Reinforcement Learning

Qingfeng Lan <sup>\*1,2</sup> A. Rupam Mahmood <sup>1,3</sup> Shuicheng Yan <sup>2</sup> Zhongwen Xu <sup>2</sup>

## Abstract

In recent years, by leveraging more data, computation, and diverse tasks, learned optimizers have achieved remarkable success in supervised learning optimization, outperforming classical hand-designed optimizers. However, in practice, these learned optimizers fail to generalize to reinforcement learning tasks due to unstable and complex loss landscapes. Moreover, neither hand-designed optimizers nor learned optimizers have been specifically designed to address the unique optimization properties in reinforcement learning. In this work, we take a data-driven approach to learn to optimize for reinforcement learning using meta-learning. We introduce a novel optimizer structure that significantly improves the training efficiency of learned optimizers, making it possible to learn an optimizer for reinforcement learning from scratch. Although trained in toy tasks, our learned optimizer demonstrates its generalization ability to unseen complex tasks. Finally, we design a set of small gridworlds to train the first general-purpose optimizer for reinforcement learning.

## 1. Introduction

Deep learning has achieved great success in many areas (Le-Cun et al., 2015), which is largely attributed to the automatically learned features that surpass handcrafted expert features. The use of gradient descent enables automatic adjustments of parameters within a model, yielding highly effective features. Despite these advancements, as another important component in deep learning, optimizers are still largely hand-designed and heavily reliant on expert knowledge, such as RMSprop (Tieleman & Hinton, 2012) and

Adam (Kingma & Ba, 2015).

To reduce the burden of hand-designing optimizers, researchers propose to learn to optimize (Sutton, 1992; Andrychowicz et al., 2016; Wichrowska et al., 2017; Maheswaranathan et al., 2021) with the help of meta-learning. A learned optimizer is typically represented by a neural network, named the meta-network. Its parameters and gradients are called meta-parameters and meta-gradients, respectively. The meta-network can be used to compute the hyper-parameters of classical optimizers (Xu et al., 2017; Metz et al., 2019) or the changes of parameters in a learning model (Lv et al., 2017; Li & Malik, 2017). During meta-learning, the meta-network is updated to achieve better optimization. For example, hyper-parameters (e.g., the learning rate) can be adjusted automatically. Even the parameter update rule can be directly learned from training data. Compared to designing optimizers with human expert knowledge, learning an optimizer is a data-driven approach, reducing the reliance on expert knowledge. Despite the significant progress made in learning optimizers, previous works only present learned optimizers under supervised learning (SL) settings. These learned optimizers usually have complex neural network structures and incorporate numerous human-designed input features, requiring a large amount of computation and human effort to design and train them. However, they have been shown to perform poorly in reinforcement learning (RL) tasks (Metz et al., 2020b; 2022b). Learning to optimize for RL remains an open and challenging problem.

Classical optimizers are typically designed for optimization in SL tasks and then applied to RL tasks. However, RL tasks possess unique properties that are largely overlooked by classical optimizers. For example, unlike SL, the input distribution of an RL agent is non-stationary and non-independent and identically distributed (non-i.i.d.) due to locally correlated transition dynamics (Alt et al., 2019). Additionally, the target function and the loss landscapes in RL are constantly changing throughout the learning process, as a result of policy and value iterations. These unique properties make the optimization process in RL much more unstable and complex. It is also inappropriate to apply optimization algorithms designed for SL to RL directly (Bengio et al., 2020a;b). Yet we still lack optimizers specifically designed for RL tasks.

<sup>\*</sup>This work was done during an internship at Sea AI Lab, Singapore. Code release: <https://github.com/sail-sg/optim4rl> <sup>1</sup>Department of Computing Science, University of Alberta, Edmonton, Alberta, Canada <sup>2</sup>Sea AI Lab, Singapore <sup>3</sup>CIFAR AI Chair, Amii. Correspondence to: Qingfeng Lan <qlan3@ualberta.ca>, Zhongwen Xu <zhongwen.s.xu@gmail.com>.

In this work, we aim to learn optimizers for RL with meta-learning. That is, instead of manually designing optimizers by studying the unique properties of RL, we apply meta-learning to learn optimizers using data generated during the interactions of agents and environments. Specifically, we present *Optim4RL*, a learned optimizer for RL. Inspired by classical adaptive optimizers, Optim4RL is designed with effective inductive biases to accelerate the learning of a good optimization method. Compared with previous works, Optim4RL is more stable to train and more effective in optimizing RL tasks, without designing complex neural network structures or incorporating numerous human-designed input features. We demonstrate that the proposed Optim4RL can learn to optimize RL tasks from scratch and generalize to unseen tasks. Finally, we design a set of gridworlds with various properties and meta-learn a general-purpose RL optimizer in these tasks. To the best of our knowledge, our work is the first one to propose an effective learned optimizer for deep RL.

## 2. Background

### 2.1. Reinforcement Learning

In reinforcement learning (RL), an agent learns by trial and error to maximize a reward signal. The process of reinforcement learning can be formalized mathematically as a Markov Decision Process (MDP). Formally, let  $M = (\mathcal{S}, \mathcal{A}, P, r, \gamma)$  be an MDP which includes a state space  $\mathcal{S}$ , an action space  $\mathcal{A}$ , a state transition probability function  $P : \mathcal{S} \times \mathcal{A} \times \mathcal{S} \rightarrow \mathbb{R}$ , a reward function  $r : \mathcal{S} \times \mathcal{A} \rightarrow \mathbb{R}$ , and a discount factor  $\gamma \in [0, 1]$ . For a given MDP, the agent interacts with the MDP according to its policy  $\pi$ , which maps a state to a distribution over the action space. At each time-step  $t$ , the agent observes a state  $S_t \in \mathcal{S}$  and samples an action  $A_t$  from  $\pi(\cdot | S_t)$ . Then it observes the next state  $S_{t+1} \in \mathcal{S}$  according to the transition function  $P$  and receives a scalar reward  $R_{t+1} = r(S_t, A_t) \in \mathbb{R}$ . The agents aim to find an optimal policy  $\pi^*$  to maximize the expectation of the return,  $G_t = \sum_{k=t}^{\infty} \gamma^{k-t} R_{k+1}$ . The state-value function  $v_{\pi}$  induced by the policy  $\pi$  maps states to expected returns. Moreover, it can be written recursively in form of a Bellman equation:  $v_{\pi}(s) = \mathbb{E}_{\pi}[R_{t+1} + \gamma v_{\pi}(S_{t+1}) | S_t = s]$ . In practice, we approximate  $v_{\pi}$  with  $v$ . The recursive form of  $v_{\pi}$  allows us to approximate  $v_{\pi}$  by bootstrapping from the current estimate of the value function  $v$ , which is also known as temporal difference (TD) learning:

$$v(S_t) \leftarrow v(S_t) + \alpha \underbrace{(R_{t+1} + \gamma v(S_{t+1}) - v(S_t))}_{\text{the TD target}}, \quad (1)$$

where  $\alpha$  is the learning rate and  $R_{t+1} + \gamma v(S_{t+1})$  is named the TD target.

### 2.2. Learning to Optimize with Meta-learning

We aim to learn an optimizer using meta-learning. Let  $\theta$  be the agent-parameters that we aim to optimize with an optimizer. A (learned) optimizer is defined as an update function  $U$  which maps input gradients to parameter updates, implemented as a meta-network, parameterized by the meta-parameters  $\phi$ . Let  $z$  be the input features which may include gradients  $g$ , losses  $L$ , and exponential moving average of gradients. Let  $h$  be an optimizer state which stores historical values. We can then compute agent-parameters updates  $\Delta\theta$  as well as the updated agent-parameters  $\theta'$  with

$$\Delta\theta, h' = U_{\phi}(z, h), \text{ and } \theta' = \theta + \Delta\theta. \quad (2)$$

Note that all classical first-order optimizers can be written in the form of Equation 2 with  $\phi = \emptyset$ . For example, in SGD,  $h' = h = \emptyset$ ,  $z = g$ , and  $U_{\text{SGD}}(g, \emptyset) = (-\alpha g, \emptyset)$ , where  $\alpha$  is the learning rate. In RMSProp (Tieleman & Hinton, 2012), let  $z = g$ , and  $h$  is used to store the average of squared gradients. Then  $U_{\text{RMSProp}}(g, h) = (-\frac{\alpha g}{\sqrt{h'+\epsilon}}, h')$ , where  $h' = \beta h + (1-\beta)g^2$ ,  $\alpha$  is the learning rate,  $\beta \in [0, 1]$ , and  $\epsilon$  is a tiny positive number for numerical stability.

Similar to Xu et al. (2020), we apply two-level optimization to optimize  $\theta$  and  $\phi$ . First, we collect a sequence of  $M + 1$  trajectories  $\mathcal{T} = \{\tau_i, \tau_{i+1}, \dots, \tau_{i+M-1}, \tau_{i+M}\}$ . For the inner update, we fix  $\phi$  and apply multiple steps of gradient descent updates to  $\theta$  by minimizing an inner loss  $L^{\text{inner}}$ . Specifically, for each trajectory  $\tau_i \in \mathcal{T}$ , we have

$$\Delta\theta_i \propto \nabla_{\theta} L^{\text{inner}}(\tau_i; \theta_i, \phi) \text{ and } \theta_{i+1} \leftarrow \theta_i + \Delta\theta_i,$$

where  $\nabla_{\theta} L^{\text{inner}}$  are agent-gradients of  $\theta$ . By repeating the above process for  $M$  times, we get  $\theta_i \xrightarrow{\phi} \theta_{i+1} \dots \xrightarrow{\phi} \theta_{i+M}$ . Here,  $\theta_{i+M}$  are actually functions of  $\phi$ . For simplicity, we abuse the notation and still use  $\theta_{i+M}$ . Next, we use  $\tau_{i+M}$  as a validation trajectory to optimize  $\phi$  with an outer loss  $L^{\text{outer}}$ :

$$\Delta\phi \propto \nabla_{\phi} L^{\text{outer}}(\tau_{i+M}; \theta_{i+M}, \phi) \text{ and } \phi \leftarrow \phi + \Delta\phi.$$

Note that  $\nabla_{\phi} L^{\text{outer}}$  are meta-gradients. Since  $\theta_{i+M}$  are functions of  $\phi$ , we can apply the chain rule to compute meta-gradients. In practice, this can be done with the help of automatic differentiation packages.

## 3. Related Work

Our work is closely related to two areas: optimization in reinforcement learning (RL) and learning to optimize in supervised learning (SL).

### 3.1. Optimization in RL

Henderson et al. (2018) tested different optimizers in RL settings and pointed out that classical adaptive optimizers may

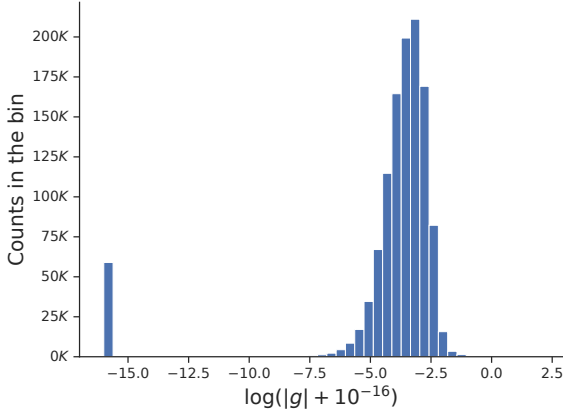


Figure 1. A visualization of agent-gradients collected during training A2C in `big_dense_long`, optimized by RMSProp. We compute  $\log(|g| + 10^{-16})$  to avoid the error of applying log function to non-positive agent-gradients. The  $y$ -axis shows the number of elements in corresponding bins.

not always consider the complex interactions between RL algorithm properties and the dynamics of the environment. Sarigül & Avci (2018) benchmarked different momentum strategies in deep RL and found that Nesterov momentum is better at generalization. Bengio et al. (2020a) took one step further and showed that unlike SL, momentum in TD learning becomes doubly stale due to changing parameter updates and bootstrapping. By correcting momentum in TD learning, the sample efficiency is improved in policy evaluation. Later, Bengio et al. (2020b) studied the connection between TD learning and generalization and interference. They found that, due to the interplay between the dynamics of interference and bootstrapping in TD learning, low-interference parameters often memorize when TD learning is involved, while low-interference parameters tend to generalize in supervised classification tasks. These works together hint that it may not always be appropriate to bring optimization methods in SL directly to RL, without considering the unique properties in RL. In this work, we adopt a data-driven approach. Instead of studying these properties and hand-designing new optimizers for RL tasks, we apply meta-learning to learn an optimizer for RL from data generated in the interactions of agents and environments.

### 3.2. Learning to Optimize in SL

Initially, learning to optimize is only applied to tune hyperparameters in classical optimizers, such as learning rates (Jacobs, 1988; Sutton, 1992; Schraudolph & Sejnowski, 1995; Mahmood et al., 2012). Recently, researchers have started to learn an optimizer completely from scratch. Andrychowicz et al. (2016) implemented learned optimizers with long short-term memory networks (LSTMs) (Hochreiter

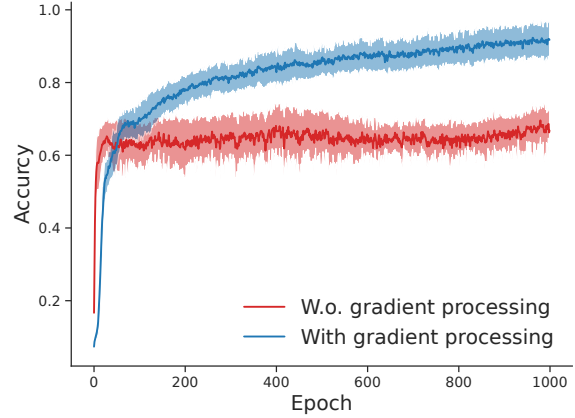


Figure 2. The accuracy of RNN models approximating the identity function, with or without gradient processing.

& Schmidhuber, 1997), trained by meta-learning. They showed that learned optimizers could generalize to similar but unseen tasks, outperforming hand-designed optimizers. Li & Malik (2017) represented an optimization method as a policy in RL and applied a guided policy search method to find a good optimizer. Wichrowska et al. (2017) introduced a novel hierarchical recurrent neural network (RNN) (Medsker & Jain, 2001) architecture, which greatly reduces memory and computation, and was shown to generalize to neural networks of different structures. They also developed a dataset consisting of small tasks with diverse loss landscapes for meta-learning. Instead of using RNNs, Metz et al. (2022a) developed learned optimizers with multi-layer perceptrons (MLPs) only, which achieves a better balance among memory, computation, and performance.

Learned optimizers are known to be hard to train. Part of the reason is that they are usually trained by truncated back-propagation through time, which leads to strongly biased gradients or exploding gradients. To overcome these issues, Metz et al. (2019) presented a method to dynamically weigh a reparameterization gradient estimator and an evolutionary strategy style gradient estimator, stabilizing the training of learned optimizers. Vicol et al. (2021) resolved the issues by dividing the computation graph into truncated unrolls and computing unbiased gradients with evolution strategies and gradient bias corrections.

Harrison et al. (2022) investigated the training stability properties of optimization algorithms with tools from dynamical systems and proposed to improve the stability of learned optimizers by adding adaptive nominal terms based on Adam (Kingma & Ba, 2015) and AggMo (Lucas et al., 2019). Metz et al. (2020a) trained a general-purpose optimizer, STAR, by training optimizers on thousands of tasks with a large amount of computation. Following the same

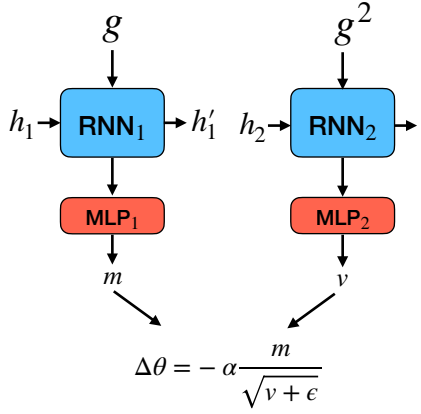


Figure 3. The network structure of Optim4RL.

spirit, Metz et al. (2022b) continued to perform large-scale optimizer training, leveraging more computation (4,000 TPU-months) and more diverse SL tasks. The learned optimizer, VeLO, requires no hyperparameter tuning and works well on a wide range of SL tasks.

VeLO is the precious outcome of long-time research in the area of learning to optimize, building on the wisdom and effort of many generations and a large amount of computation. Although marking a milestone for the success of learned optimizers in SL tasks, VeLO still performs poorly in RL tasks, as shown in Section 4.4.4 in Metz et al. (2022b). The failure of VeLO in RL tasks suggests that designing learned optimizers for RL tasks is still a challenging problem.

Note that all previously mentioned works focus on training learned optimizers for SL. Our work is inspired by them but focuses on learning to optimize for RL. Compared to these works, our method (i.e., Optim4RL) is simple, stable, and effective, without using complex neural network structures or incorporating numerous human-designed input features. As far as we know, our work is the first to demonstrate the success of learned optimizers in deep RL.

#### 4. Learning to Optimize in RL is Much Harder

In supervised learning (SL), a training dataset consists of pairs  $\{(x_i, y_i)\}$  where  $x_i$  is the input and  $y_i$  is the label for input  $x_i$ . The goal is to train a model that maps the input data to the correct labels. During training, a mini-batch is sampled from the dataset and fed into the model to generate predictions  $\hat{y}_s$  for input  $x_s$ . A loss is computed given the predicted labels  $\hat{y}_s$  and the true labels  $y_s$ . A lower loss usually indicates better performance (e.g., higher classification accuracy). The parameters of this model are then optimized given the loss function with gradient descent

methods. Note that in the training process, it is assumed that the training set consists of i.i.d. samples. Moreover, the true labels  $y_s$  are usually noiseless and stationary (i.e., time-invariant). For example, the true label of a written digit 2 in MNIST (Deng, 2012) is always  $y = 2$  which does not change during training.

However, in reinforcement learning (RL), the input training data distribution is non-i.i.d., which makes the whole training process much more unstable and complex, especially when learning to optimize is involved. Compared with SL, one significant difference in RL training is that the agent-environment interactions change input data distribution, such as visited states and rewards. TD learning is widely used in RL, and TD targets (see Equation 1) in RL play a similar role as labels in SL. However, unlike labels in SL, TD targets are usually biased, non-stationary, and noisy due to changing state-values, complex state transitions, and noisy reward signals. This leads to a changing loss landscape that evolves as the policy and the state-value function change. Unlike SL, a lower loss is not necessarily a good indicator of better performance (i.e., higher return) in RL for this reason. The randomness from state transitions, reward signals, and agent-environment interactions, together with biased TD targets, makes the bias and variance of agent-gradients relatively high.

Learned optimizers for SL are infamously hard to train, suffering from high training instability (Wichrowska et al., 2017; Metz et al., 2019; 2020a; Harrison et al., 2022). Learning an optimizer for RL tasks is even harder, due to the high bias and variance of agent-gradients in RL. During learning to optimize in RL, meta-gradients are afflicted with large noise induced by the high bias and variance of agent-gradients. Since meta-gradients are noisy and inaccurate, the improvement of the learned optimizer becomes unstable and slow. With a poorly performed optimizer, the agent policy improvement is no longer guaranteed. Due to the agent-environment interactions, a poor agent policy is unlikely to collect “high-quality” data to boost the performance of both the agent and the learned optimizer. In the end, this two-level optimization gets stuck in a vicious spiral: a poor optimizer  $\rightarrow$  a poor agent policy  $\rightarrow$  collected data of low-quality  $\rightarrow$  a poor optimizer  $\rightarrow \dots$ . Note that this phenomenon also occurs to learning to optimize in SL. It is the agent-gradients of high bias and variance in RL and the agent-environment interactions that make learning to optimize in RL much harder.

#### 5. Optim4RL: A Learned Optimizer for RL

To overcome the hardness of learning an optimizer in RL, we introduce a dual-RNN structure optimizer, named *Optim4RL*, that is more robust and sample-efficient than previous methods. To achieve this, we first employ a technique

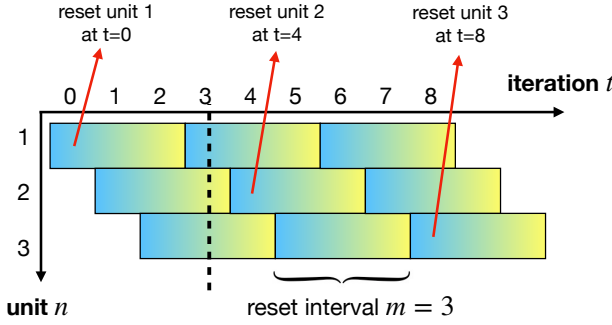


Figure 4. An illustration of pipeline training where reset interval  $m = 3$  and the number of units  $n = 3$ . All training units are reset at regular intervals to diversify input training data.

for generating improved gradient representations, which is crucial for the success of Optim4RL. We then describe the key features in the network structure of Optim4RL.

### 5.1. Gradient Processing

Before feeding agent-gradients into neural networks, we process them to get new gradient representations. Specifically, for each scalar gradient  $g$ , we map it into a pair of real values:

$$g \rightarrow [\text{sgn}(g), \log(|g| + \varepsilon)] \quad (3)$$

where  $\varepsilon$  is a small value to prevent the error of computing  $\log(0)$ . In this work, we set it to  $10^{-18}$  in all experiments. We find that gradient processing significantly improves the training stability and performance of learned optimizers. Note that there is a similar gradient processing method proposed in Andrychowicz et al. (2016). However, we find our approach is simpler and better in practice.

In Figure 1, we visualize collected agent-gradients during training A2C (Mnih et al., 2016) in a gridworld, optimized by RMSProp (Tieleman & Hinton, 2012). The gridworld is named `big_dense_long` (see the appendix for details) in which the agent is required to move and collect objects. We plot these agent-gradients with logarithmic  $x$ -axis. The  $y$ -axis shows the number of elements in corresponding bins. Notice that the agent-gradients vary across a wide range in logarithms, from  $-\infty$  (we truncate it to  $-16$  in the plot) to 0, while their absolute values are in a small range (i.e., in  $[0, 1]$ ). This requires a learned optimizer to distinguish small value differences between agent-gradients in order to generate accurate parameter updates. Furthermore, there are two peaks in the distribution, which makes it harder to approximate an optimizer update function with neural networks. By transforming  $g$  to  $[\text{sgn}(g), \log(|g| + \varepsilon)]$ , neural networks would be able to recover  $g$  since no information is lost. The new gradient representations also allow neural networks to distinguish small value differences of agent-

gradients due to the log function.

Surprisingly, we find that it is hard for RNNs to approximate the identity function without gradient processing. Consider the identity function  $f(g) = g$  where  $g$  is the input agent-gradient. This is a special case that a learned optimizer approximates SGD with a learning rate  $-1$ . We train two RNN models to approximate the identity function for 1,000 epochs by minimizing the mean squared error  $(\hat{g} - g)^2$ , where  $\hat{g}$  is the predicted value. Each RNN model consists of an LSTM and an MLP with two hidden layers of size 16, with or without gradient processing. We measure model performance by accuracy. Specifically, the model makes a correct prediction if  $\min((1 - \epsilon')g, (1 + \epsilon')g) \leq \hat{g} \leq \max((1 - \epsilon')g, (1 + \epsilon')g)$  where  $\epsilon' = 0.1$ ; otherwise,  $\hat{g}$  is a wrong prediction. We plot the training accuracies of two approaches, averaging over 10 runs. As shown in Figure 2, there is a large performance gap between the two approaches, showing the advantage of gradient processing. Moreover, we find that the convergence accuracy with gradient processing is slightly above 90%, far from 100%. This result again validates the difficulty of learning a good optimizer: it is hard for RNN models to approximate the identity function accurately, let alone learn a much more complex parameter update function.

### 5.2. A Dual-RNN Structure

In general, we want to learn a good update function in a reasonable hypothesis space. This hypothesis space should be large enough to include as many good known optimizers as possible, such as Adam (Kingma & Ba, 2015) and RMSProp (Tieleman & Hinton, 2012). Meanwhile, we should also rule out obviously bad choices so that a good candidate can be found efficiently during training. Inspired by the success of classical optimizers, we parameterize the parameter update function in a similar form to adaptive optimizers (i.e., Adam, RMSProp, etc.):

$$\Delta\theta = -\alpha \frac{m}{\sqrt{v + \epsilon}}, \quad (4)$$

where  $\alpha$  is the learning rate,  $\epsilon$  is a small positive value, and  $m$  and  $v$  are the processed outputs of two RNNs followed by two MLPs, as shown in Figure 3.

In practice, it is very hard for neural networks to approximate mathematical operations accurately without additional techniques involved (Telgarsky, 2017; Yarotsky, 2017; Boullé et al., 2020; Lu et al., 2021). Besides applying gradient preprocessing, we mitigate this issue by building inductive biases into the design of learned optimizers. By parameterizing the parameter update function as Equation 4, we reduce the burden of approximating square root and division for neural networks. Note that we also test another

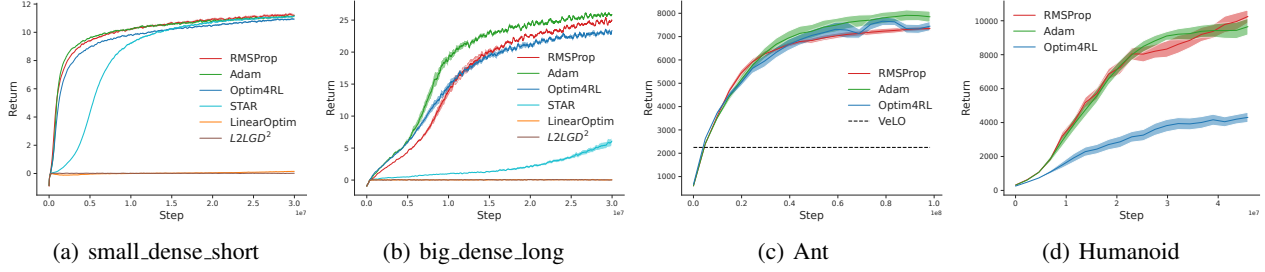


Figure 5. The optimization performance of different optimizers. Note that the performance of VeLO is estimated based on Figure 11(a) in Metz et al. (2022b), shown as a dashed line. All other results are averaged over 10 runs, where the shaded areas represent standard errors.

learned optimizer with a “linear” parameter update function:

$$\Delta\theta = -\alpha(a * g + b), \quad (5)$$

where  $\alpha$  is the learning rate,  $a$  and  $b$  are the processed outputs of one RNN followed by one MLP. We name this optimizer *LinearOptim*, which also incorporates gradient processing. Note that L2LGD<sup>2</sup>, a method proposed by Andrychowicz et al. (2016), is a special case of LinearOptim, where  $b \equiv 0$ . Both LinearOptim and L2LGD<sup>2</sup> fail even in simple gridworlds, as we will show next. Considering the failures of LinearOptim and L2LGD<sup>2</sup> validate, we choose to apply a dual-RNN structure in Optim4RL, with its advantage validated in experiments.

Finally, besides gradients, many previously learned optimizers for SL include human-designed features as inputs, such as moving average of gradient values at multiple timescales, moving average of squared gradients, and Adafactor-style accumulators (Shazeer & Stern, 2018). Including human-designed features not only makes the optimizer more complex but is also against the goal of learning to optimize. Ideal learned optimizers should be able to automatically learn useful features, reducing the reliance on human expert knowledge as much as possible. Unlike these optimizers, we only consider gradients as inputs for simplicity. In theory, the above input features (i.e., exponential moving average of gradient values at multiple timescales, etc.) can be learned and stored in the hidden states of RNNs. As we will show next, despite its simplicity, our learned optimizer achieves significantly better performance in RL tasks, compared to learned optimizers for SL. Following Andrychowicz et al. (2016), our optimizer operates coordinatewisely on agent parameters, which means that all agent-parameters share the same optimizer.

## 6. Experiment

In this section, we first design experiments to verify that Optim4RL can be learned from scratch in RL tasks. Then we investigate the generalization ability of Optim4RL in different RL tasks. Based on the insights from the inves-

tigation, we show how to train a general-purpose learned optimizer for RL that generalizes to complex RL tasks.

Similar to Oh et al. (2020), we design 8 gridworlds with diverse properties: small\_sparse\_short, small\_sparse\_long, small\_dense\_long, big\_sparse\_short, big\_spare\_long, big\_dense\_short, small\_dense\_short, and big\_dense\_long. These gridworlds are designed to be different regarding horizons, reward functions, and state-action spaces. The details of all gridworlds are described in the appendix. Besides gridworlds, we also test our method in several Brax tasks (Freeman et al., 2021). We mainly consider two RL algorithms — A2C (Mnih et al., 2016) and PPO (Schulman et al., 2017). For all experiments, we train A2C in gridworlds and train PPO in Brax tasks.

For Optim4RL, we use two GRUs (Cho et al., 2014) with hidden size 8; both MLPs have two hidden layers with size 16. To meta-learn optimizers, we set  $M = 4$  in all experiments; that is, for every outer update, we do inner update 4 times. We use Adam as the meta-optimizer to optimize learned optimizers. We compare Optim4RL with two classical optimizers, Adam and RMSProp. For A2C, the inner loss is the standard A2C loss, while the outer loss is the actor loss in A2C loss. For PPO, both the inner loss and outer loss are the standard PPO loss. Please check the appendix for more implementation details.

### 6.1. Learning an Optimizer for RL from Scratch

In this section, we show that it is feasible to train Optim4RL in RL tasks from scratch, and that directly applying learned optimizers for SL to optimize in RL tasks does not work, especially for hard RL tasks.

Specifically, two easy gridworlds (small\_dense\_short and big\_dense\_long) and two complex Brax tasks (Ant and Humanoid) are selected as test environments. Besides Adam and RMSProp, we consider three other baselines: L2LGD<sup>2</sup> (Andrychowicz et al., 2016), a classical learned optimizer in SL; STAR (Harrison et al., 2022) and VeLO (Metz et al., 2022b), two state-of-the-art learned optimizers in SL.

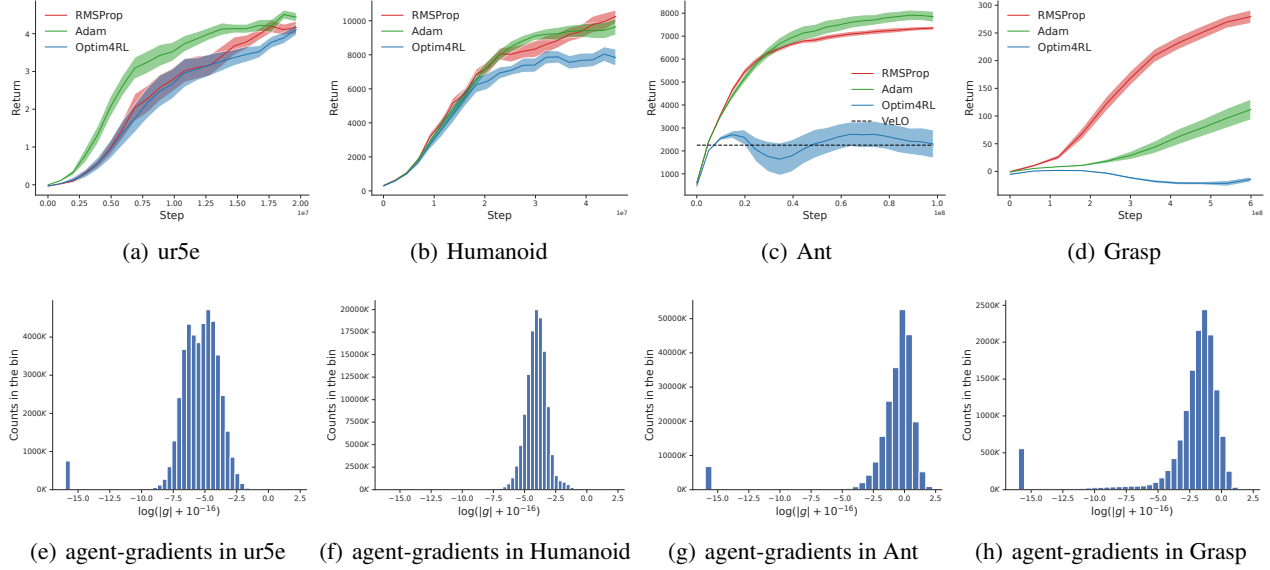


Figure 6. (a-d) The optimization performance of Optim4RL in four Brax tasks, averaged over 10 runs with the shaded areas representing standard errors. This Optim4RL only trained in `big_dense_long`. The performance of VeLO is estimated based on Figure 11(a) in [Metz et al. \(2022b\)](#), shown as a dashed line. (e-h) The agent-gradients collected during training PPO in each task, optimized by RMSProp.

In general, a good optimizer should be well-functioned across the whole training stage. To achieve that, we propose *pipeline training*. To be specific, we train  $n$  agents at the same time, each with its own task and optimizer state. Together they form a training unit (agent, task, optimizer state), and we have  $n$  training units in total. Let  $m$  be a positive integer we call *reset interval*. For unit  $i \in \{1, \dots, n\}$ , we assign an integer  $r_i$  to it, where  $r_1, \dots, r_n$  are chosen so that they are evenly spaced over the interval  $[0, m - 1]$ . At training iteration  $t = 0, 1, \dots$ , we reset the agent-parameters, the task, and the optimizer state of training unit  $i$ , where  $t \equiv r_i \pmod{m}$ . In Figure 4, we show a special case of pipeline training where  $m = n = 3$ . By resetting each training unit at regular intervals, pipeline training guarantees that at any iteration  $t$  (e.g., at  $t = 3$ , the dashed line in Figure 4), we can get access to training data across one training interval for meta-learning. In practice, we find that pipeline training greatly increases the training stability and efficiency of learned optimizers.

We apply pipeline training to meta-learn optimizers in one task and then test the fixed learned optimizers in this specific task. We compare the optimization performance of different optimizers and plot the learning curves in Figure 5, averaging over 10 runs. In `small_dense_short`, Optim4RL and STAR perform quite well, on par with Adam and RMSProp. However, in `big_dense_long`, which is a harder task with a larger state-action space than `small_dense_short`, STAR fails to optimize effectively, and the return increases slowly as training proceeds. In both `small_dense_short` and `big_dense_long`, LinearOptim (see Equation 5) and L2LGD<sup>2</sup> fail to optimize, proving the im-

portance of the dual-RNN structure in Optim4RL. In Ant, Optim4RL performs similarly to Adam and RMSProp, significantly outperforming VeLO. In Humanoid, though Optim4RL is no better than RMSProp and Adam, the learning curve has a good increasing trend. Note that due to memory constraint, we only train Optim4RL to optimize a much smaller PPO network than the standard one used in Brax ([Freeman et al., 2021](#)). This might be one of the reasons that Optim4RL does not perform well in Humanoid.

## 6.2. Investigating Generalization Ability of Optim4RL

To test the generalization ability of Optim4RL, we apply a learned Optim4RL trained in `big_dense_long` from Section 6.1 in four Brax tasks, shown in Figure 6 (a-d). Although the learned Optim4RL is trained in a much simpler task (i.e., `big_dense_long`), it still generalizes to two unseen complex Brax games — ur5e and Humanoid, but fails in Ant and Grasp. To investigate, we plot the agent-gradients during training PPO in each Brax game in Figure 6 (e-h). Note that all agents are optimized with RMSProp<sup>1</sup>. Comparing the agent-gradient distributions in Figure 1 and Figure 6 (e-h), we find that there is a large distribution overlap between the collected agent-gradients in `big_dense_long` and the ones in ur5e. Same for Humanoid but not for Ant or Grasp. This aligns with a straightforward intuition: a learned optimizer is unlikely to perform well in unseen gradient distributions. In other words, a learned optimizer can only generalize to tasks with similar agent-gradient distributions.

<sup>1</sup>The agent-gradient distributions optimized by Adam are also similar to Figure 6 (e-h).

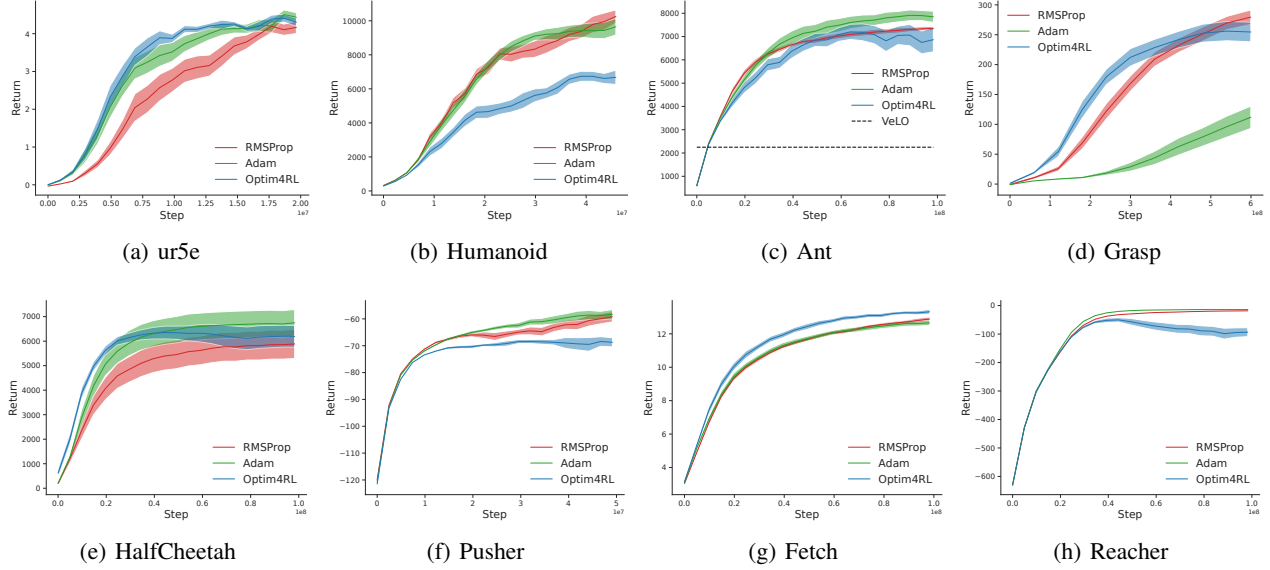


Figure 7. Optim4RL generalizes to 8 Brax tasks successfully. Note that the performance of VeLO is estimated based on Figure 11(a) in Metz et al. (2022b), shown as a dashed line. All other results are averaged over 10 runs with the shaded areas representing standard errors. Optim4RL is trained in 6 selected gridworlds, showing a strong generalization ability.

### 6.3. Toward a General-Purpose Learned Optimizer for Reinforcement Learning

The insight from the previous section points out a promising approach to learning a general-purpose optimizer for RL: meta-train learned optimizers in multiple RL tasks with various agent-gradient distributions. The key challenge is to design tasks with various agent-gradient distributions. We find that, by changing the reward scale in a gridworld, the agent-gradient distribution in that gridworld would change accordingly. For example, by using a reward function that is 10 times the original reward function, the new agent-gradients shift toward large values. So we choose 6 gridworlds and carefully tune reward scales for these tasks such that the union of all agent-gradients covers a large range. We list the selected gridworlds as well as their corresponding reward scales and agent learning rates in Table 1.

The scales of meta-gradients generated in different gridworlds are quite different. Following Metz et al. (2022b), we normalize meta-gradients of each task to be unit-length before averaging them across different tasks. We save trained meta-parameters in different training stages and test them in 8 Brax tasks: ur5e, Humanoid, Ant, Grasp, HalfCheetah, Pusher, Fetch, and Reacher. In Figure 7, we show the optimization performance of the best-learned optimizer. All results are averaged over 10 runs, and the shaded areas represent standard errors. Our learned optimizer Optim4RL surpasses VeLO significantly in Ant. Compared with Adam and RMSProp, Optim4RL outperforms them in Fetch; matches Adam and RMSProp in ur5e, Ant, Grasp, and HalfCheetah. And it performs slightly worse in Humanoid, Pusher, and

Table 1. The selected gridworlds with their corresponding reward scales and learning rates (LR) for learning a general-purpose optimizer.

Gridworld	Reward Scale	LR
small_dense_long	1000	1e-3
small_dense_short	100	3e-3
big_sparse_short	100	3e-3
big_dense_short	10	3e-3
big_sparse_long	10	1e-3
big_dense_long	1	3e-3

Reacher. In general, Optim4RL is competitive compared with classical human-designed optimizers, even though it is entirely trained from scratch in toy tasks.

## 7. Conclusion and Future Work

In this work, we presented the first general-purpose learned optimizer for RL tasks — Optim4RL. Optim4RL is designed to have strong inductive biases and a novel network structure, achieving higher training stability and better performance than learned optimizers in SL. We showed that by training Optim4RL entirely from scratch in toy tasks, it is able to generalize to complex RL tasks and matches the performance of classical hand-designed optimizers.

Though achieving great success, the current result is still limited since Optim4RL is only trained in a small number of toy tasks. In addition, we only considered two on-policy RL algorithms, A2C and PPO. Similar to Metz et al. (2022b), by

leveraging more computation and memory, it is promising to extend our approach to a larger scale, training Optim4RL with thousands of different RL agents in diverse tasks.

## References

Alt, B., Šošić, A., and Koepll, H. Correlation priors for reinforcement learning. *Advances in Neural Information Processing Systems*, 32, 2019.

Andrychowicz, M., Denil, M., Gomez, S., Hoffman, M. W., Pfau, D., Schaul, T., Shillingford, B., and De Freitas, N. Learning to learn by gradient descent by gradient descent. *Advances in Neural Information Processing Systems*, 2016.

Bengio, E., Pineau, J., and Precup, D. Correcting momentum in temporal difference learning. *NeurIPS Workshop on Deep RL*, 2020a.

Bengio, E., Pineau, J., and Precup, D. Interference and generalization in temporal difference learning. In *International Conference on Machine Learning*, 2020b.

Boullé, N., Nakatsukasa, Y., and Townsend, A. Rational neural networks. *Advances in Neural Information Processing Systems*, 33:14243–14253, 2020.

Cho, K., van Merriënboer, B., Bahdanau, D., and Bengio, Y. On the properties of neural machine translation: Encoder–decoder approaches. In *Proceedings of SSST-8, Eighth Workshop on Syntax, Semantics and Structure in Statistical Translation*, 2014.

Deng, L. The MNIST database of handwritten digit images for machine learning research. *IEEE Signal Processing Magazine*, 2012.

Freeman, C. D., Frey, E., Raichuk, A., Girgin, S., Mordatch, I., and Bachem, O. Brax - a differentiable physics engine for large scale rigid body simulation, 2021. URL <https://github.com/google/brax>.

Harrison, J., Metz, L., and Sohl-Dickstein, J. A closer look at learned optimization: Stability, robustness, and inductive biases. In *Advances in Neural Information Processing Systems*, 2022.

Henderson, P., Romoff, J., and Pineau, J. Where did my optimum go?: An empirical analysis of gradient descent optimization in policy gradient methods. In *The 14th European Workshop on Reinforcement Learning*, 2018.

Hochreiter, S. and Schmidhuber, J. Long short-term memory. *Neural computation*, 1997.

Jacobs, R. A. Increased rates of convergence through learning rate adaptation. *Neural Networks*, 1988.

Kingma, D. P. and Ba, J. Adam: A method for stochastic optimization. In *International Conference on Learning Representations*, 2015.

LeCun, Y., Bengio, Y., and Hinton, G. Deep learning. *Nature*, 2015.

Li, K. and Malik, J. Learning to optimize. In *International Conference on Learning Representations*, 2017.

Lu, L., Jin, P., Pang, G., Zhang, Z., and Karniadakis, G. E. Learning nonlinear operators via DeepONet based on the universal approximation theorem of operators. *Nature Machine Intelligence*, 2021.

Lucas, J., Sun, S., Zemel, R., and Grosse, R. Aggregated momentum: Stability through passive damping. In *International Conference on Learning Representations*, 2019.

Lv, K., Jiang, S., and Li, J. Learning gradient descent: Better generalization and longer horizons. In *International Conference on Machine Learning*, 2017.

Maheswaranathan, N., Sussillo, D., Metz, L., Sun, R., and Sohl-Dickstein, J. Reverse engineering learned optimizers reveals known and novel mechanisms. *Advances in Neural Information Processing Systems*, 2021.

Mahmood, A. R., Sutton, R. S., Degris, T., and Pilarski, P. M. Tuning-free step-size adaptation. In *2012 IEEE International Conference on Acoustics, Speech and Signal Processing (ICASSP)*, 2012.

Medsker, L. R. and Jain, L. Recurrent neural networks. *Design and Applications*, 2001.

Metz, L., Maheswaranathan, N., Nixon, J., Freeman, D., and Sohl-Dickstein, J. Understanding and correcting pathologies in the training of learned optimizers. In *International Conference on Machine Learning*, 2019.

Metz, L., Maheswaranathan, N., Freeman, C. D., Poole, B., and Sohl-Dickstein, J. Tasks, stability, architecture, and compute: Training more effective learned optimizers, and using them to train themselves. *arXiv preprint arXiv:2009.11243*, 2020a.

Metz, L., Maheswaranathan, N., Sun, R., Freeman, C. D., Poole, B., and Sohl-Dickstein, J. Using a thousand optimization tasks to learn hyperparameter search strategies. *arXiv preprint arXiv:2002.11887*, 2020b.

Metz, L., Freeman, C. D., Harrison, J., Maheswaranathan, N., and Sohl-Dickstein, J. Practical tradeoffs between memory, compute, and performance in learned optimizers. In *Conference on Lifelong Learning Agents*, 2022a.

Metz, L., Harrison, J., Freeman, C. D., Merchant, A., Beyer, L., Bradbury, J., Agrawal, N., Poole, B., Mordatch, I., Roberts, A., et al. VeLO: Training versatile learned optimizers by scaling up. *arXiv preprint arXiv:2211.09760*, 2022b.

Mnih, V., Badia, A. P., Mirza, M., Graves, A., Lillicrap, T., Harley, T., Silver, D., and Kavukcuoglu, K. Asynchronous methods for deep reinforcement learning. In *International conference on machine learning*, 2016.

Oh, J., Hessel, M., Czarnecki, W. M., Xu, Z., van Hasselt, H. P., Singh, S., and Silver, D. Discovering reinforcement learning algorithms. *Advances in Neural Information Processing Systems*, 2020.

Sarıgil, M. and Avci, M. Performance comparison of different momentum techniques on deep reinforcement learning. *Journal of Information and Telecommunication*, 2018.

Schraudolph, N. and Sejnowski, T. J. Tempering backpropagation networks: Not all weights are created equal. *Advances in Neural Information Processing Systems*, 1995.

Schulman, J., Wolski, F., Dhariwal, P., Radford, A., and Klimov, O. Proximal policy optimization algorithms. *arXiv preprint arXiv:1707.06347*, 2017.

Shazeer, N. and Stern, M. Adafactor: Adaptive learning rates with sublinear memory cost. In *International Conference on Machine Learning*, 2018.

Sutton, R. S. Adapting bias by gradient descent: An incremental version of delta-bar-delta. In *Proceedings of the AAAI Conference on Artificial Intelligence*, 1992.

Telgarsky, M. Neural networks and rational functions. In *International Conference on Machine Learning*, 2017.

Tieleman, T. and Hinton, G. Lecture 6.5-RMSProp: Divide the gradient by a running average of its recent magnitude. *COURSERA Neural Networks Neural Networks for Machine Learning*, 2012.

Vicol, P., Metz, L., and Sohl-Dickstein, J. Unbiased gradient estimation in unrolled computation graphs with persistent evolution strategies. In *International Conference on Machine Learning*, 2021.

Wichrowska, O., Maheswaranathan, N., Hoffman, M. W., Colmenarejo, S. G., Denil, M., Freitas, N., and Sohl-Dickstein, J. Learned optimizers that scale and generalize. In *International Conference on Machine Learning*, 2017.

Xu, C., Qin, T., Wang, G., and Liu, T.-Y. Reinforcement learning for learning rate control. *arXiv preprint arXiv:1705.11159*, 2017.

Xu, Z., van Hasselt, H. P., Hessel, M., Oh, J., Singh, S., and Silver, D. Meta-gradient reinforcement learning with an objective discovered online. *Advances in Neural Information Processing Systems*, 2020.

Yarotsky, D. Error bounds for approximations with deep ReLU networks. *Neural Networks*, 2017.

## A. Gridworlds

We follow Oh et al. (2020) and design 8 gridworlds. In each gridworld, there are  $N$  objects. Each object is described as  $[r, \epsilon_{\text{term}}, \epsilon_{\text{respawn}}]$ . Object locations are randomly determined at the beginning of each episode, and an object reappears at a random location after being collected, with a probability of  $\epsilon_{\text{respawn}}$  for each time-step. The observation consists of a tensor  $\{0, 1\}^{N \times H \times W}$ , where  $N$  is the number of objects, and  $H \times W$  is the size of the grid. An agent has 9 movement actions for adjacent positions, including staying in the same position. When the agent collects an object, it receives the corresponding reward  $r$ , and the episode terminates with a probability of  $\epsilon_{\text{term}}$  associated with the object.

In the following tables, we describe each gridworld in detail.

Table 2. small\\_sparse\\_short

Component	Description
Size ( $H \times W$ )	$3 \times 8$
Objects	$[1.0, 0.0, 0.05], [-1.0, 0.5, 0.05]$
Horizon	50

Table 3. small\\_sparse\\_long

Component	Description
Size ( $H \times W$ )	$8 \times 3$
Objects	$[1.0, 0.0, 0.05], [-1.0, 0.5, 0.05]$
Horizon	500

Table 4. small\\_dense\\_short

Component	Description
Size ( $H \times W$ )	$4 \times 6$
Objects	$[1.0, 0.0, 0.5], [-1.0, 0.5, 0.5]$
Horizon	50

Table 5. small\_dense\_long

Component	Description
Size ( $H \times W$ )	$6 \times 4$
Objects	$[1.0, 0.0, 0.5], [-1.0, 0.5, 0.5]$
Horizon	500

Table 6. big\_sparse\_short

Component	Description
Size ( $H \times W$ )	$10 \times 12$
Objects	$2 \times [1.0, 0.0, 0.05], 2 \times [-1.0, 0.5, 0.05]$
Horizon	50

Table 7. big\_sparse\_long

Component	Description
Size ( $H \times W$ )	$12 \times 10$
Objects	$2 \times [1.0, 0.0, 0.05], 2 \times [-1.0, 0.5, 0.05]$
Horizon	500

Table 8. big\_dense\_short

Component	Description
Size ( $H \times W$ )	$9 \times 13$
Objects	$2 \times [1.0, 0.0, 0.5], 2 \times [-1.0, 0.5, 0.5]$
Horizon	50

Table 9. big\_dense\_long

Component	Description
Size ( $H \times W$ )	$13 \times 9$
Objects	$2 \times [1.0, 0.0, 0.5], 2 \times [-1.0, 0.5, 0.5]$
Horizon	500